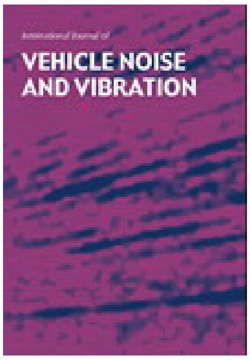

International Journal of Vehicle Noise and Vibration

ISSN online: 1479-148X - ISSN print: 1479-1471
https://www.inderscience.com/ijvnv

Preview control of the random response of a full car vehicle model traversing a rough road

L.V.V. Gopala Rao, V.S.V. Satyanarayana, Rakesh Chandmal Sharma, Srihari Palli, Anuj Raturi, Ashwani Kharola, Ashwini Sharma

DOI: 10.1504/IJVNV.2023.10062219

Article History:

Received:	29 November 2022
Last revised:	22 June 2023
Accepted:	03 August 2023
Published online:	29 April 2024

Preview control of the random response of a full car vehicle model traversing a rough road

L.V.V. Gopala Rao

Veneklasen Associates India LLP,
Gurgaon, Haryana, India
Email: lvvgrao@gmail.com

V.S.V. Satyanarayana

Mechanical Engineering Department,
Vignan's Institute of Information Technology,
Visakhapatnam, India
Email: svajrapu18@gmail.com

Rakesh Chandmal Sharma*

Department of Mechanical Engineering,
Graphic Era (Deemed to be University),
Dehradun, India
and
Department of Mechanical Engineering,
Graphic Era Hill University,
Dehradun, India
Email: rcsharmaiitr@gmail.com
*Corresponding author

Srihari Palli

Department of Mechanical Engineering,
Aditya Institute of Technology and Management,
Tekkali, India
Email: srihari.palli@gmail.com

Anuj Raturi, Ashwani Kharola and Ashwini Sharma

Department of Mechanical Engineering,
Graphic Era (Deemed to be University),
Dehradun, India
Email: anujraturi@geu.ac.in
Email: ashwanikharola.me@geu.ac.in
Email: ashwinisharma.me@geu.ac.in

Abstract: This paper considers a full-vehicle model with preview control travelling on a random road. The road roughness is modelled as the PSD of the random road irregularity provided by integrated white noise which is estimated by a deterministic step input. The response of the vehicle model is optimised to improve the vehicle performance given by a performance index which is the weighted integral of suspension working space, tyre deflection and control force. The RMS values of control force, suspension space and tyre deflection are computed using the method of spectral decomposition. The results show that there is a substantial improvement in the vehicle performance in the case of linear-quadratic regulator with preview control compared to the linear-quadratic regulator without preview control.

Keywords: full vehicle model; random road; active suspension; preview control; spectral decomposition.

Reference to this paper should be made as follows: Gopala Rao, L.V.V., Satyanarayana, V.S.V., Sharma, R.C., Palli, S., Raturi, A., Kharola, A. and Sharma, A. (2024) 'Preview control of the random response of a full car vehicle model traversing a rough road', *Int. J. Vehicle Noise and Vibration*, Vol. 20, No. 1, pp.70–88.

Biographical notes: L.V.V. Gopala Rao is PhD from the Indian Institute of Technology Madras and MTech from the Andhra University, Visakhapatnam. Formerly, he was a Professor in Mechanical Engineering, Vignan's Institute of Information Technology Visakhapatnam. His area of research is vehicle dynamics and mechanical vibrations.

V.S.V. Satyanarayana holds a PhD from the Jawaharlal Nehru Technological University, Kakinada and an Associate Professor in Mechanical Engineering, Vignan's Institute of Information Technology Visakhapatnam. His area of research is vehicle dynamics and mechanical vibrations.

Rakesh Chandmal Sharma holds a PhD from the Indian Institute of Technology Roorkee and MTech from the Indian Institute of Technology BHU Varanasi. He has around 100 research articles in SCIE/ESCI/Scopus indexed journals. His area of research is vehicle dynamics and mechanical vibrations. He has 25 years of teaching experience.

Srihari Palli holds a PhD from the Andhra University, Visakhapatnam and MTech from the Indian Institute of Technology Roorkee. His area of research is vehicle dynamics and mechanical vibrations. He has 17 years of teaching experience.

Anuj Raturi is an Assistant Professor and pursuing PhD from the Department of Mechanical Engineering, Graphic Era (Deemed to be University) Dehradun, India. He is a registered Indian Patent Agent and an IP practitioner since 2012. He has having 12 years of teaching experience.

Ashwani Kharola is an Assistant Professor and a Doctorate from the Graphic Era (Deemed to be University) Dehradun, India. He has worked as Post-doctoral Fellow at Association of Indian Universities, New Delhi.

Ashwini Sharma holds a PhD from the National Institute of Technology, Kurukshetra and certified for CMI Level 5 in Management and Leadership from the Chartered Management Institute, UK. He has 25 years of teaching experience.

1 Introduction

In recent years, the design of active and semi-active vehicle suspension systems for better comfort has been one of the vital research areas when analysing vehicle vibration: Qatu et al. (2009), Qatu (2012), Sharma (2017), Sharma et al. (2020), Palli and Ramji (2015) and Tseng and Hrovat (2015). Active suspension systems use actuators that generate a controlled force counteracting the external excitation as a function of vehicle response. Many authors have done research in the active suspension field and shown that the preview control in an active control scheme improves vehicle performance well: Birla and Swarup (2015), Gong et al. (2011) and Paden et al. (2016). A quarter vehicle model has been considered with the active suspension problem design in stochastic optimal control format for direct computation of vehicle response has been formulated in the past: Nagarkar et al. (2018). Thompson and Pearce (2001) derived a faster and easier method for estimating the performance index in the case of a quarter-car vehicle model with limited road preview. This method is extended to a half-vehicle model for computing the performance index: Thompson and Davis (2003). A more concise way of computing the performance index, root mean square (RMS) values of control force, wheel travel and tyre deflection was demonstrated by Thompson and Pearce (2003). In a further development, a spectral decomposition method was used for computing the RMS values accurately for the control force, suspension space and tyre deflection of half vehicle model: Thompson and Davis (2005). A nonlinear half-vehicle model with a preview is considered and its random response is obtained by the spectral decomposition technique: Gopala Rao and Narayana (2008). There is a significantly improved performance observed in the front wheel responses with an increased preview distance and it saturates after a particular preview distance. The rear-wheel road holding response is observed almost the same as the front-wheel road holding response. Prabakar et al. (2009) used a preview-based H-∞ active control system and obtained the optimal response of a semi-active controlled magnetorheological half-car model. The sky-hook controller as a feedback controller and the preview data as a feed-forward control for improving ride comfort has been used by researchers: Göhrle et al. (2014). Wu et al. (2017) derived the augmented error methodology for the design of an optimal preview controller and presented the tracking responses of the controller with preview and non-preview with a reference signal. The implementation of preview control in tracked vehicle active suspension has been investigated in the past: Youn et al. (2017). These authors proposed a method for estimating the road disturbance data at the front wheel and utilised this information for controlling the following wheels of the vehicle. A quarter-car vehicle with a single-degree-of-freedom seat suspension model for improving ride quality has been analysed in the past: Alfadhli et al. (2018). This study, it is proposed a cost-effective control method in which the preview information was taken from the vehicle suspension dynamics instead of from a road profile. A pre-determined feedback-based static preview controller was proposed and results show that the proposed controller yields sub-optimal performance: Hamada (2019). A remarkable variety of actuators and advanced control schemes have evolved over the last few years to improve ride comfort and handling: Bhardawaj et al. (2020), Sharma and Sharma (2019), Palli et al. (2021) and Sharma et al. (2021b, 2021c). Many of the studies considered quarter or half-car vehicle models in the design of the active control suspension systems. But in reality, it is more appropriate to consider the bounce, pitch and roll motions of the vehicle in the design of active suspension controllers: Gupta et al. (2016), León-Vargas et al. (2018) and Haddar et al. (2021).

In recent years, full-vehicle models have been used in the design and analysis of vehicle suspension control systems. Pedro et al. (2018) considered a full vehicle model to design an intelligent controller and carried out the robustness analysis for parameter variations and disturbances. A genetic algorithm for determining the optimum proportional integrator multi input multi output controller tuning parameters for a full car lab setup model with active suspension has also been applied in the past: Haemers et al. (2018). Jing et al. (2018) designed a robust *H*-∞ controller for reducing the vibration disturbance to the passengers in the specified frequency range. They adopted a full vehicle model for the controller design and the variations in the suspension parameters are included in the study. As compared to quarter or half-car, a full-car vehicle model considers the roll dynamics and therefore considers the influence of the anti-roll bars as well. A half-car model can consider the pitching effect but not the roll: Desai et al. (2021), Sharma et al. (2021a). Several researchers have used different active control strategies with full car models for the improvement of ride control, stability and vehicle performance in the past: Göhrle et al. (2013, 2014, 2015), Kim et al. (2002), Ulsoy et al. (2012) and Youn et al. (2014).

In this study, the preview active suspension control of a full vehicle model has been investigated for overall response control of bouncing, pitching and rolling motions simultaneously. The vehicle's response to random road action is optimised based on preview control. The choice of optimal preview control is concerned with operating a dynamic system at a minimum cost. The previous investigations suggest that preview control is capable of reducing the vertical acceleration of the vehicle's centre of gravity with optimal control thus providing better ride comfort as compared with non-preview suspension control. The road is formulated as a result of first-order filtered random white noise. Using the spectral decomposition method with minimum computational effort, the suspension control force, tyre deflection and wheel suspension travel and passenger riding comfort are computed for the full vehicle model. The realisation of preview control strength on the full vehicle suspension performance under random road excitation is the novel part of this work.

2 Dynamic equations of motion of a full vehicle model

The full-vehicle model is shown in Figure 1.

The equations for the considered model are written as:

- For vehicle body bounce motion,

$$M\ddot{y}_c = U_1 + U_2 + U_3 + U_4 \tag{1}$$

- For vehicle body pitching motion,

$$I_{yy}\ddot{\theta} = -(U_1 + U_2)a + (U_3 + U_4)b \tag{2}$$

- For vehicle body rolling motion,

$$I_{xx}\ddot{\phi} = (U_2 + U_4)_d - (U_1 + U_3)c \tag{3}$$

- For front right wheel,

$$m_1 \ddot{y}_1 = -k_{tr_1}\left(y_1 - h_{f_1}\right) - U_1 \tag{4}$$

- For front left wheel,

$$m_2 \ddot{y}_3 = -k_{tf_1}\left(y_3 - h_{f_2}\right) - U_2 \tag{5}$$

- For rear right wheel,

$$m_3 \ddot{y}_5 = -k_{tr_2}\left(y_5 - h_{r_1}\right) - U_3 \tag{6}$$

- For rear left wheel,

$$m_4 \ddot{y}_7 = -k_{tf_2}\left(y_7 - h_{r_2}\right) - U_4 \tag{7}$$

$$\ddot{y}_2 = \ddot{y}_c - a\ddot{\theta} - c\ddot{\phi}$$

$$\ddot{y}_2 = \alpha_1 U_1 + \beta_1 U_2 + \beta_2 U_3 + \beta_3 U_4 \tag{8}$$

$$\ddot{y}_4 = \ddot{y}_c - a\ddot{\theta} + d\ddot{\phi}$$

$$\ddot{y}_4 = \beta_1 U_1 + \alpha_2 U_2 + \beta_3 U_3 + \beta_4 U_4 \tag{9}$$

$$\ddot{y}_6 = \ddot{y}_c + b\ddot{\theta} - c\ddot{\phi}$$

$$\ddot{y}_6 = \beta_2 U_1 + \beta_3 U_2 + \alpha_3 U_3 + \beta_5 U_4 \tag{10}$$

$$\ddot{y}_8 = \ddot{y}_c + b\ddot{\theta} + b\ddot{\phi}$$

$$\ddot{y}_8 = \beta_3 U_1 + \beta_4 U_2 + \beta_5 U_3 + \alpha_4 U_4 \tag{11}$$

where

$$\alpha_1 = \frac{1}{m} + \frac{a^2}{I_{yy}} + \frac{c^2}{I_{xx}};\ \alpha_2 = \frac{1}{m} + \frac{a^2}{I_{yy}} + \frac{d^2}{I_{xx}};$$

$$\alpha_3 = \frac{1}{m} + \frac{b^2}{I_{yy}} + \frac{c^2}{I_{xx}};\ \alpha_4 = \frac{1}{m} + \frac{b^2}{I_{yy}} + \frac{d^2}{I_{xx}};$$

$$\beta_1 = \frac{1}{m} + \frac{a^2}{I_{yy}} - \frac{cd}{I_{xx}};\ \beta_2 = \frac{1}{m} - \frac{ab}{I_{yy}} + \frac{c^2}{I_{xx}};$$

$$\beta_3 = \frac{1}{m} - \frac{ab}{I_{yy}} - \frac{cd}{I_{xx}};\ \beta_4 = \frac{1}{m} - \frac{ab}{I_{yy}} + \frac{d^2}{Ixx};$$

$$\beta_5 = \frac{1}{m} + \frac{b^2}{I_{yy}} - \frac{cd}{I_{xx}}.$$

Figure 1 Full-car model

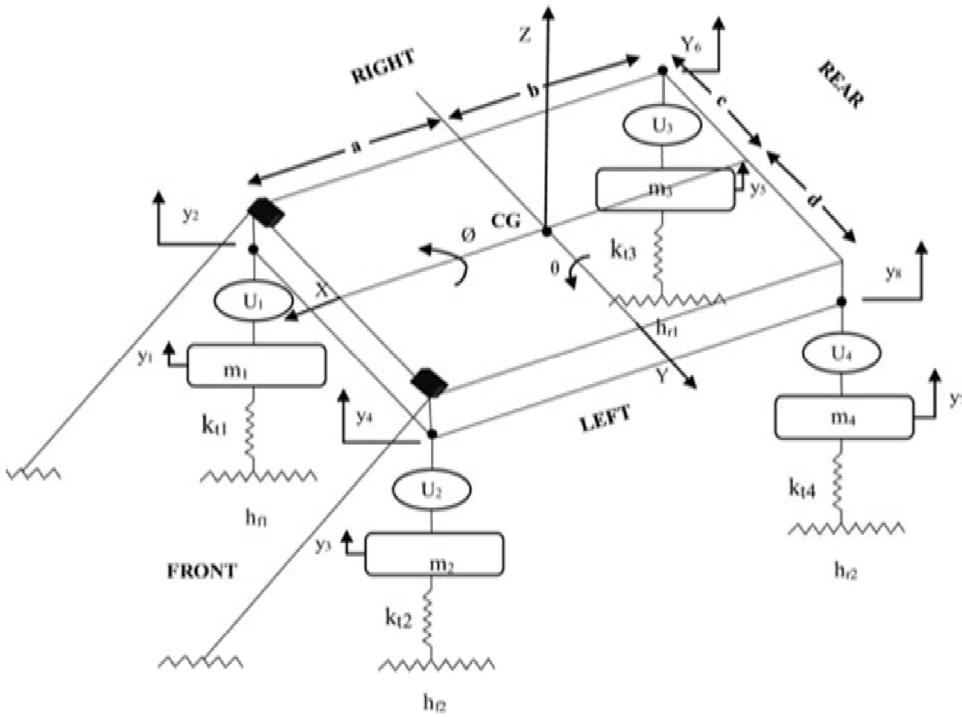

2.1 State-space conceptualisation

Representing the equations (1)–(7) in state-space model,

$$\dot{z} = Az + Ku + R\dot{w} \tag{12}$$

where

$$z = \begin{bmatrix} z_1 & z_2 & z_3 & z_4 & z_5 & \dots & \dots & \dots & \dots & z_{15} & z_{16} \end{bmatrix}^T \tag{13}$$

with

$z_1 = y_1 - h_{f1}$; $z_2 = y_2 - y_1$;

$z_3 = y_9 = \dot{y}_1$; $z_4 = y_{10} = \dot{y}_2$;

$z_5 = y_3 - h_{f2}$; $z_6 = y_4 - y_3$;

$z_7 = y_{11} = \dot{y}_3$; $z_8 = y_{12} = \dot{y}_4$;

$z_9 = y_5 - h_{r1}$; $z_{10} = y_6 - y_5$;

$z_{11} = y_{13} = \dot{y}_5$; $z_{12} = y_{14} = \dot{y}_6$;

$z_{13} = y_7 - h_{r2}$; $z_{14} = y_8 - y_7$;

$$z_{15} = y_{15} = \dot{y}_7;\ z_{16} = y_{16} = \dot{y}_8;$$

$$\dot{y}_1 = y_9;\ \dot{y}_2 = y_{10};\ \dot{y}_3 = y_{11};\ \dot{y}_4 = y_{12};$$

$$\dot{y}_5 = y_{13};\ \dot{y}_6 = y_{14};\ \dot{y}_7 = y_{15};\ \dot{y}_8 = y_{16}.$$

A, K and R are the matrices for the vectors describing the system, control force and road input respectively. $z(t)$, $u(t)$ and $w(t)$ are the matrices for the system state, controlling force and white noise vectors. The vectors are as follows:

$$A = \begin{bmatrix} A_1 & A_2 \\ A_3 & A_4 \end{bmatrix}$$

$$A_1 = \begin{bmatrix} 0 & 0 & 1 & 0 & 0 & 0 & 0 & 0 \\ 0 & 0 & -1 & 1 & 0 & 0 & 0 & 0 \\ -\dfrac{k_{tr_1}}{m_1} & 0 & 0 & 0 & 0 & 0 & 0 & 0 \\ 0 & 0 & 0 & 0 & 0 & 0 & 0 & 0 \\ 0 & 0 & 0 & 0 & 0 & 0 & 1 & 0 \\ 0 & 0 & 0 & 0 & 0 & 0 & -1 & 1 \\ 0 & 0 & 0 & 0 & \dfrac{-k_{tf_1}}{m_2} & 0 & 0 & 0 \\ 0 & 0 & 0 & 0 & 0 & 0 & 0 & 0 \end{bmatrix}$$

$$A_2 = [0]_{8\times 8};\ A_3 = [0]_{8\times 8}$$

$$A_4 = \begin{bmatrix} 0 & 0 & 1 & 0 & 0 & 0 & 0 & 0 \\ 0 & 0 & -1 & 1 & 0 & 0 & 0 & 0 \\ -\dfrac{k_{tr_2}}{m_3} & 0 & 0 & 0 & 0 & 0 & 0 & 0 \\ 0 & 0 & 0 & 0 & 0 & 0 & 0 & 0 \\ 0 & 0 & 0 & 0 & 0 & 0 & 1 & 0 \\ 0 & 0 & 0 & 0 & 0 & 0 & -1 & 1 \\ 0 & 0 & 0 & 0 & \dfrac{-k_{tf_2}}{m_4} & 0 & 0 & 0 \\ 0 & 0 & 0 & 0 & 0 & 0 & 0 & 0 \end{bmatrix}$$

$$k=\begin{bmatrix} 0 & 0 & \frac{1}{m_1} & \alpha_1 & 0 & 0 & 0 & \beta_1 & 0 & 0 & 0 & \beta_2 & 0 & 0 & 0 & \beta_3 \\ 0 & 0 & 0 & \beta_1 & 0 & 0 & \frac{-1}{m_2} & \alpha_2 & 0 & 0 & 0 & \beta_3 & 0 & 0 & 0 & \beta_4 \\ 0 & 0 & 0 & \beta_2 & 0 & 0 & 0 & \beta_3 & 0 & 0 & \frac{-1}{m_3} & \alpha_3 & 0 & 0 & 0 & \beta_5 \\ 0 & 0 & 0 & \beta_3 & 0 & 0 & 0 & \beta_4 & 0 & 0 & 0 & \beta_5 & 0 & 0 & \frac{-1}{m_4} & \alpha_4 \end{bmatrix}$$

$$R=\begin{bmatrix} -1 & 0 & 0 & 0 & 0 & 0 & 0 & 0 & 0 & 0 & 0 & 0 & 0 & 0 & 0 & 0 \\ 0 & 0 & 0 & 0 & -1 & 0 & 0 & 0 & 0 & 0 & 0 & 0 & 0 & 0 & 0 & 0 \\ 0 & 0 & 0 & 0 & 0 & 0 & 0 & 0 & -1 & 0 & 0 & 0 & 0 & 0 & 0 & 0 \\ 0 & 0 & 0 & 0 & 0 & 0 & 0 & 0 & 0 & 0 & 0 & 0 & -1 & 0 & 0 & 0 \end{bmatrix}$$

$$\dot{w}=\left[\dot{h}_{f1}\dot{h}_{f2}\dot{h}_{r1}\dot{h}_{r2}\right]^T$$

$$u=\left[U_1U_2U_3U_4\right]$$

$$h_f=f\left(t-T_1\right)$$

$$h_f=f\left(t-T_2\right)$$

where T_1 and T_2 are preview time and wheelbase preview time; h_f and h_r represent front and rear wheel unit step road inputs.

Power spectral density (PSD) of the random road profile is considered as expressed in Thompson and Davis (2005)

$$\Phi(\omega)=\frac{cV}{\omega^2}, \tag{14}$$

where c is the constant corresponding to the roughness of a given road, ω and V denote angular frequency and vehicle velocity. The RMS response of the considered model to the unit step input can be obtained by using this relation is considered as given in Davis and Thompson (2001).

From now on, the state vector $z(t)$ corresponding to step input will be taken equivalent to the response of the system to random excitation input.

The RMS values of $z(t)$ and $u(t)$ can be expressed as considered as expressed by Thompson and Pearce (2001).

$$\left\langle z(t)z^T(t)\right\rangle=2\pi cV\int_0^\infty z(t)z^T(t)dt \tag{15}$$

$$\left\langle u(t)u^T(t)\right\rangle=2\pi cV\int_0^\infty u(t)u^T(t)dt \tag{16}$$

3 Solution of optimal preview controller equations for a full vehicle model using spectral decomposition analysis

The objective is to optimise the system regarding the minimisation of the weighted sum of suspension stroke, road holding and control force at the front and rear wheels.

The overall performance index is expressed by,

$$\begin{aligned} J = \int_0^\infty \Big[& \rho_1 u_1^2 + \rho_2 u_2^2 + \rho_3 u_3^2 + \rho_4 u_4^2 + q_1 \left(y_1 - h_{f_1} \right)^2 \\ & + q_2 \left(y_1 - y_2 \right)^2 + q_3 \left(y_3 - h_{f_2} \right)^2 + q_4 \left(y_4 - y_3 \right)^2 \\ & + q_5 \left(y_5 - h_{r_1} \right)^2 + q_6 \left(y_6 - y_5 \right)^2 \\ & + q_7 \left(y_7 - h_{r_2} \right)^2 + q_8 \left(y_8 - y_7 \right)^2 \Big] dt \end{aligned} \tag{17}$$

where ρ_1, ρ_2, ρ_3, ρ_4, q_1, q_2, q_3, q_4, q_5, q_6, q_7 and q_8 are weighting factors selected.

The performance index is written in matrix form as

$$J = \int_0^\infty \left(zQz^T + uBu^T \right) dt, \tag{18}$$

where

$$Q = diag\left[q_1 q_2 \quad 0 \quad 0 \quad q_3 q_4 \quad 0 \quad 0 \quad q_5 q_6 \quad 0 \quad 0 \quad q_7 q_8 \right]$$

$$B = diag\left[\rho_1 \rho_2 \rho_3 \rho_4 \right]$$

Preview control force,

$$u(t) = u_b z(t) + u_f r(t) \tag{19}$$

Feedback and feed-forward components u_b and u_f are given by,

$$u_b = -B^{-1} K^T S \tag{20}$$

$$u_f = -B^{-1} K^T \tag{21}$$

and S is derived by solving the matrix Riccati equation,

$$A^T S + SA - SKB^{-1} KS + Q = 0 \tag{22}$$

On substitution of equations (19)–(21) in equation (12),

$$\dot{z} = A_c z - KB^{-1} K^T r(t) + R\dot{w} \tag{23}$$

$$A_c = A - KB^{-1} K^T S \tag{24}$$

In equation (19), $r(t)$ can be written as,

$$\dot{r} = A_c r + SR\dot{w} = 0 \tag{25}$$

The solution of the equation (25) is given as

$$\begin{aligned} r(t) &= \int_0^{\infty} \exp\left(A_c^T(t-\tau)\right) SR\dot{w}(\tau)d\tau \\ &= e^{A_c^T(T_1-\tau)} Sd_1 U\left(T_1 - t\right) + e^{A_c^T(T_1-\tau)} Sd_2 U\left(T_1 - t\right) \\ &\quad + e^{A_c^T(T_2-\tau)} Sd_3 U\left(T_2 - t\right) + e^{A_c^T(T_2-\tau)} Sd_4 U\left(T_2 - t\right) \end{aligned} \tag{26}$$

Equations (23) and (25) are expressed as,

$$\begin{bmatrix} \dot{z} \\ \dot{r} \end{bmatrix} = \begin{bmatrix} A_c & -KB^{-1}K^T \\ 0 & -A_c^T \end{bmatrix} \begin{bmatrix} z \\ r \end{bmatrix} + \begin{bmatrix} R \\ -SR \end{bmatrix} \dot{w}. \tag{27}$$

Writing the equations in diagonal form, eigenvalues and eigenvectors can be evaluated as follows.

$$\begin{bmatrix} A_c & KB^{-1}K^T \\ 0 & -A_c^T \end{bmatrix} \begin{bmatrix} V_{11} & V_{12} \\ 0 & V_{22} \end{bmatrix} = \begin{bmatrix} V_{11} & V_{11} \\ 0 & V_{22} \end{bmatrix} \begin{bmatrix} \lambda & 0 \\ 0 & -\lambda \end{bmatrix} \tag{28}$$

Now, submatrix A_c written in spectral decomposition form as $V_{11}^{-1} A_c V_{11} = \lambda$.

Let $V_{11}^{-1} = U_{11}$ and

$$\begin{bmatrix} x_a \\ x_b \end{bmatrix} = \begin{bmatrix} U_{11} & U_{12} \\ 0 & U_{22} \end{bmatrix} \begin{bmatrix} z \\ r \end{bmatrix} \tag{29}$$

by substituting equation (29) in equation (27),

$$\begin{bmatrix} \dot{x}_a \\ \dot{x}_b \end{bmatrix} = \begin{bmatrix} \lambda & 0 \\ 0 & \lambda \end{bmatrix} \begin{bmatrix} x_a \\ x_b \end{bmatrix} + \begin{bmatrix} U_{11} & U_{12} \\ 0 & U_{22} \end{bmatrix} \begin{bmatrix} R \\ -SR \end{bmatrix} \dot{w} \tag{30}$$

The solution of equation (30) is obtained as

$$\begin{bmatrix} x_a \\ x_b \end{bmatrix} = \begin{bmatrix} e^{\lambda t} & 0 \\ 0 & -e^{\lambda t} \end{bmatrix} \left(\begin{aligned} & \begin{bmatrix} x_{0a} \\ x_{0b} \end{bmatrix} + \begin{bmatrix} x_{1a} \\ x_{1b} \end{bmatrix} h_f\left(t - T_1\right) + \begin{bmatrix} x_{2a} \\ x_{2b} \end{bmatrix} h_f\left(t - T_1\right) \\ & + \begin{bmatrix} x_{3a} \\ x_{3b} \end{bmatrix} h_r\left(t - T_2\right) + \begin{bmatrix} x_{4a} \\ x_{4b} \end{bmatrix} h_r\left(t - T_2\right) \end{aligned} \right) \tag{31}$$

where $h(t)$ represents the unit step function.

From equation (26), using $A_c^T = V_{22} \lambda U_{22}$, we get

$$\begin{aligned} r(0) &= e^{A_c^T T_1} Sd_1 + e^{A_c^T T_1} Sd_2 + e^{A_c^T T_2} Sd_3 + e^{A_c^T T_2} Sd_4 \\ &= V_{22} e^{\lambda T_1} U_{22} Sd_1 + V_{22} e^{\lambda T_1} U_{22} Sd_2 + V_{22} e^{\lambda T_1} U_{22} Sd_3 \\ &\quad + V_{22} e^{\lambda T_1} U_{22} Sd_4 \end{aligned} \tag{32}$$

and

$$\begin{bmatrix} x_{0a} \\ x_{0b} \end{bmatrix} = \begin{bmatrix} U_{12} V_{22} \left(e^{\lambda T_1} U_{22} Sd_1 + e^{\lambda T_2} U_{22} Sd_2 \right) \\ e^{\lambda T_1} U_{22} Sd_1 + e^{\lambda T_2} U_{22} Sd_2 \end{bmatrix}$$

$$\begin{bmatrix} x_{1a} \\ x_{1b} \end{bmatrix} = \begin{bmatrix} e^{-\lambda T_1}\left(U_{11} - U_{12}S\right) d_1 \\ \left(e^{-\lambda T_1} U_{22} S\right) d_1 \end{bmatrix}$$

$$\begin{bmatrix} x_{2a} \\ x_{2b} \end{bmatrix} = \begin{bmatrix} e^{-\lambda T_1}\left(U_{11} - U_{12}S\right) d_2 \\ \left(e^{-\lambda T_1} U_{22} S\right) d_2 \end{bmatrix}$$

$$\begin{bmatrix} x_{3a} \\ x_{3b} \end{bmatrix} = \begin{bmatrix} e^{-\lambda T_2}\left(U_{11} - U_{12}S\right) d_3 \\ \left(e^{-\lambda T_2} U_{22} S\right) d_3 \end{bmatrix}$$

$$\begin{bmatrix} x_{4a} \\ x_{4b} \end{bmatrix} = \begin{bmatrix} e^{-\lambda T_2}\left(U_{11} - U_{12}S\right) d_4 \\ \left(e^{-\lambda T_2} U_{22} S\right) d_4 \end{bmatrix}$$

The direct way of computing $z(t)$ and $u(t)$ are obtained analytically as follows:

To compute the matrix P_{yy}

$$P_{xx} = \int_0^\infty x(t)x^\dagger(t)dt = \int_0^\infty \begin{bmatrix} x_a(t) \\ x_b(t) \end{bmatrix} \begin{bmatrix} x_a^\dagger(t) & x_b^\dagger(t) \end{bmatrix} dt, \tag{33}$$

where '†' is the complex conjugate transpose.

The elements in the above matrix are calculated by

$$P_{xx}(i, j) = \int_0^\infty x(i)x*(j)dt, \tag{34}$$

where * denotes complex conjugate.

The above equation is written as,

$$\begin{aligned} P_{xx}(i, j) = \int_0^\infty e^{\lambda_i t} \big(&x_0(i) + x_1(i)U(t-T_1) + x_2(i)U(t-T_1) \\ &+ x_3(i)U(t-T_2) + x_4(i)U(t-T_2)\big) X \\ &\left(\left(x_0^*(j) + x_1^*(j)U(t-T_1) + x_2^*(j)U(t-T_1)\right.\right. \\ &\left.\left.+ x_3^*(j)U(t-T_2) + x_4^*(j)(t-T_2)\right)\right) e^{\lambda_j^* t} dt \end{aligned} \tag{35}$$

The equation (35) can be written as

$$P_{xx}(i, j) = \frac{1}{\lambda_i + \lambda_j}\left(P_0 + P_1 + P_2 + P_3 + P_4\right) \tag{36}$$

$$P_0 = x_0(i)x_0^*(j)$$

$$\begin{aligned} P_1 &= x_0(i)x_1^*(j) + x_0(i)x_2^*(j) \\ &\quad + \left(x_1(i) + x_2(i)\right)\left(x_0^i(j) + x_1^*(j) + x_2^*(j)\right) \end{aligned}$$

$$\begin{aligned} P_2 &= x_3(i)x_5^*(j) + x_5(i)x_3^*(j) + x_4(i)x_5^*(j) + x_5(i)x_4^*(j) \\ &\quad - x_3(i)x_3^*(j) - x_4(i)x_3^*(j) - x_4(i)x_4^*(j) \end{aligned}$$

where $x_5^* = x_0(i) + x_1(i) + x_2(i) + x_3(i) + x_4(i)$.

The equation (29) is written as

$$\begin{bmatrix} z \\ r \end{bmatrix} = \begin{bmatrix} V_{11} & V_{12} \\ 0 & V_{22} \end{bmatrix} \begin{bmatrix} x_a \\ x_b \end{bmatrix}. \tag{37}$$

From the equation (35), the mean squared z(t),

$$P_{zz} = 2\pi C_{sd} V p_{zz} \tag{38}$$

where

$$p_{zz} = \int_0^\infty zz^\dagger dt = \begin{bmatrix} V_{11} & V_{12} \end{bmatrix} P_{xx} \begin{bmatrix} V_{11}^\dagger \\ V_{22}^\dagger \end{bmatrix}. \tag{39}$$

From equation (16), preview control optimal force,

$$u = -B^{-1} G^T L^T \begin{bmatrix} x_a \\ x_b \end{bmatrix}, \tag{40}$$

where $L = [SV_{11}SV_{12} + V_{22}]$.

The mean squared control force,

$$P_{uu} = 2\pi C_{sd} V p_{uu}, \tag{41}$$

where

$$p_{uu} = \left\lceil -B^{-1} K^T L P_{xx} L^\dagger K B^{-1} \right\rceil. \tag{42}$$

4 Results and discussion

The following parameters for vehicle and road models are considered as an example.

$$\begin{aligned} &M = 1{,}136 \text{ kg}, I_{xx} = 2{,}400 \text{ kgm}^2, I_{yy} = 400 \text{ kgm}^2, m_1 = 63\ kg, m_2 = 63 \text{ kg}, \\ &m_3 = 60 \text{ kg}, m_4 = 60 \text{ kg}, k_{tf_1} = k_{tf_2} = k_{tr_1} = k_{tr_2} = 182{,}470 \text{ N/m}, a = 1.15 \text{ m}, \\ &b = 1.65 \text{ m}, c = 0.505 \text{ m}, d = 0.557 \text{ m}, c = 10^{-5}\ m, q_1 = q_2 = q_5 = q_6 = 10^6, \\ &q_9 = q_{10} = q_{13} = q_{14} = 10^6, \rho_1 = \rho_2 = \rho_3 = \rho_4 = 0.5. \end{aligned}$$

In Figure 2, the performance index is plotted for preview distances (0 and 2 m) at different speeds. It is observed from figure that performance improves as preview distance increases and saturates after a certain preview distance. Therefore, a limited preview distance exists after which the advantage of the preview control is saturated.

Figure 3 shows the RMS bounce acceleration response of sprung mass with preview and without preview for different speeds of the vehicle. It can be observed that the bounce acceleration response improves with the look-ahead control compared to the response without look-ahead control. The bounce acceleration performance improves as the preview distance increases, but it saturates beyond a particular preview distance.

Figure 4 shows RMS pitch acceleration values as a function of the velocity of the vehicle at $P_d = 0$ and $P_d = 2$ m. It is seen that preview control has a substantial effect on pitch acceleration at all velocities.

Figure 2 Performance index variation with velocity at $P_d = 0$ and $P_d = 2$ m (see online version for colours)

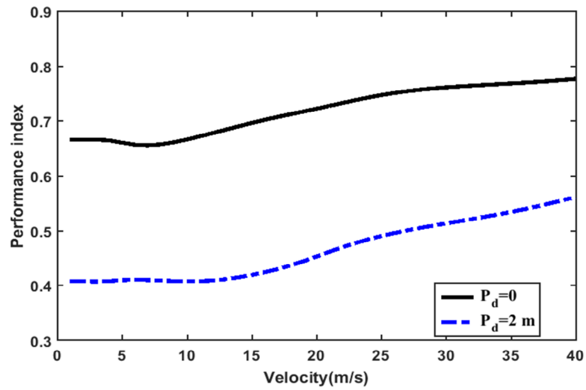

Figure 3 Comparison of RMS sprung mass bounce acceleration between preview and non-preview cases at different velocities (see online version for colours)

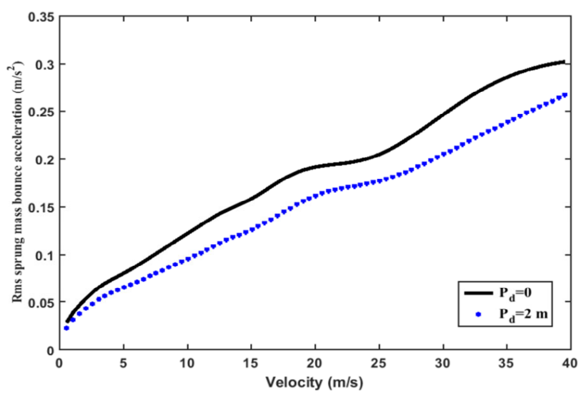

Figure 4 Comparison of RMS pitch acceleration between preview and non-preview cases at different velocities (see online version for colours)

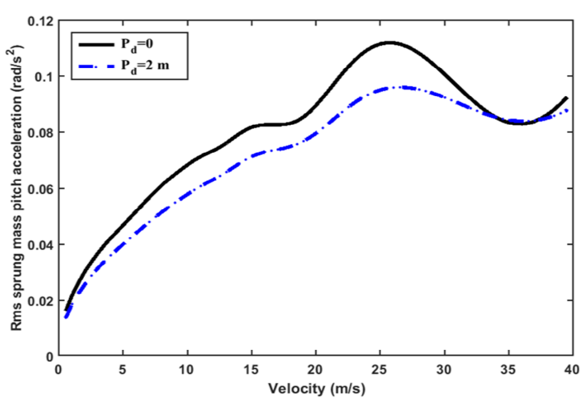

Figure 5 Comparison of RMS roll acceleration between preview and non-preview cases at different velocities (see online version for colours)

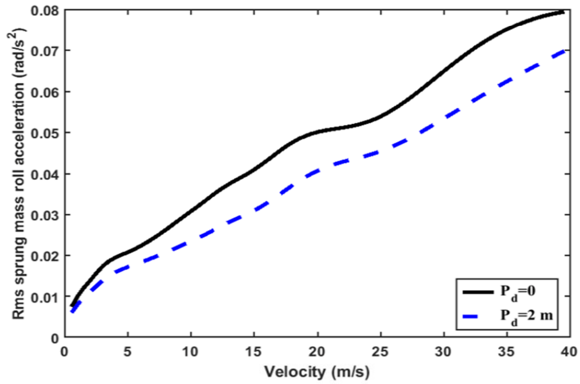

Figure 6 Comparison of RMS road holding between preview and non-preview cases for the left wheels at different velocities (see online version for colours)

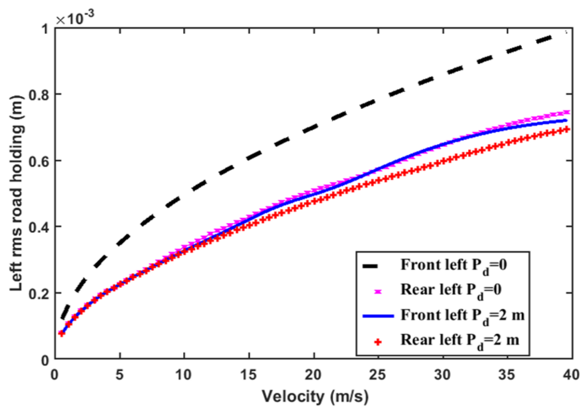

Figure 7 Comparison of RMS road holding between preview and non-preview cases for the right wheels at different velocities (see online version for colours)

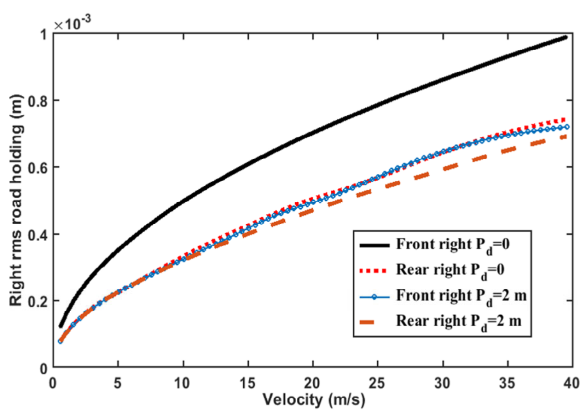

Figure 8 Comparison of RMS road suspension stroke between preview and non-preview cases for the left wheels at different velocities (see online version for colours)

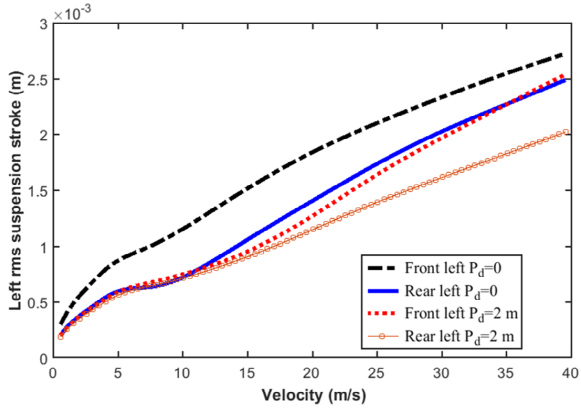

Figure 9 Comparison of RMS suspension stroke between preview and non-preview cases for the right wheels at different velocities (see online version for colours)

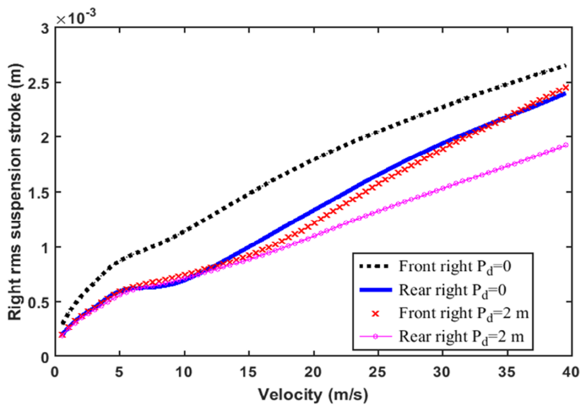

Figure 10 Variation of RMS control force at left with velocity (see online version for colours)

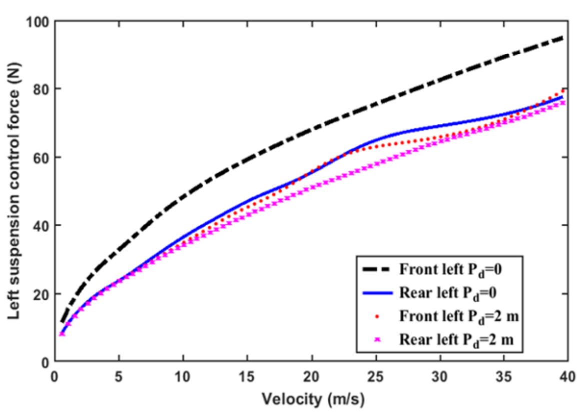

Figure 11 Variation of RMS control force at right with velocity (see online version for colours)

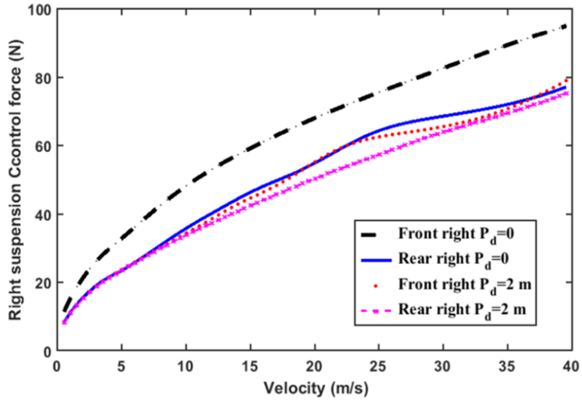

Figure 5 shows RMS roll acceleration as the function of the velocity of the vehicle for the preview and non-preview cases. It is seen that roll acceleration performance improves substantially with the preview control at all velocities.

The road-holding responses at the left and right wheels are shown in Figures 6 and 7. The rear wheels exhibit good road-holding performance when compared with the front wheel response. The preview control (p_d = 2 m) effect on the performance of front-wheel road holding is improved significantly when compared to the front-wheel road-holding performance without preview control. The rear wheel road-holding performance is improved marginally with preview control (p_d = 2 m).

In Figures 8 and 9, the suspension stroke responses at left and right tyres are plotted. The response of the rear wheels is good when compared with front-wheel response. The front wheels stroke performance is greatly improved with the preview control at all velocities. The preview control effect on the rear wheel suspension stroke response is similar as seen in the case of road-holding performance.

The left and right suspension forces are plotted at different velocities for preview and non-preview cases in Figures 10 and 11. The left and right suspension control forces of the vehicle with preview control are reduced considerably when compared with the control force of the vehicle without preview. The reason could be that the control force is one of the terms in the performance index which is minimised as per the preview control law. The front and rear wheel control forces with preview control are less compared to the control forces of the vehicle without preview.

5 Conclusions

The response of a seven-degree-of-freedom full car model active preview control suspension system has been studied for overall performance improvement of the vehicle suspension system. Random road input is equivalently modelled with unit step inputs. The spectral decomposition method was used to reduce the computational effort to determine the vehicle response and control forces. Using preview control improves overall vehicle performance compared to the non-preview control. However, the benefit of the preview control is saturated beyond a particular preview distance. The vehicle's bouncing, pitching and rolling comfort has been significantly improved. Preview control also improves the response, such as front tyres road holding, rear tyres road holding, front wheels suspension stroke, and rear-wheel suspension stroke of the vehicle. It is seen that the better performance of the preview control system is more pronounced in response to the front wheels compared to the response of the rear wheels.

References

Alfadhli, A., Darling, J. and Hillis, A.J. (2018) 'The control of an active seat with vehicle suspension preview information', *Journal of Vibration and Control*, Vol. 24, No. 8, pp.1412–1426.

Bhardawaj, S., Sharma, R.C. and Sharma, S.K. (2020) 'Development of multibody dynamical using MR damper based semi-active bio-inspired chaotic fruit fly and fuzzy logic hybrid suspension control for rail vehicle system', *Proc. I Mech. E Part K: J. Multi-body Dynamics*, Vol. 234, No. 4, pp.723–744.

Birla, N. and Swarup, A.A. (2015) 'Optimal preview control: a review', *Optim. Control Appl. Methods*, Vol. 36, No. 2, pp.241–268.

Davis, B.R. and Thompson, A.G. (2001) 'Power spectral density of road profiles', *Vehicle System Dynamics*, Vol. 35, No. 6, pp.409–415.

Desai, R., Guha, A. and Seshu, P. (2021) 'A comparison of quarter, half and full car models for predicting vibration attenuation of an occupant in a vehicle', *Journal of Vibration Engineering & Technologies*, Vol. 9, pp.983–1001.

Göhrle, C., Schindler, A., Wagner, A. and Sawodny, O. (2013) 'Model predictive control of semi-active and active suspension systems with available road preview', in *2013 European Control Conference, ECC 2013*, pp.1499–1504.

Göhrle, C., Schindler, A., Wagner, A. and Sawodny, O. (2014) 'Design and vehicle implementation of preview active suspension controllers', *IEEE Transactions on Control Systems Technology*, Vol. 22, No. 3, pp.1135–1142.

Göhrle, C., Schindler, A., Wagner, A. and Sawodny, O. (2015) 'Road profile estimation and preview control for low-bandwidth active suspension systems', *IEEE/ASME Transactions on Mechatronics*, Vol. 20, No. 5, pp.2299–2310.

Gong, D., Zhou, J., Sun, W. and Goodall, R. (2011) 'Effects of active primary suspension on vertical ride quality control of flexible car body and its comparison with those of active secondary suspension', *Proceedings of the 22nd International Symposium on Dynamics of Vehicles on Roads Tracks (IAVSD 2011)*, Vol. 1, No. 1, pp.1–6.

Gopala Rao, L.V.V. and Narayana, S. (2008) 'Preview control of random response of a half-car vehicle model traversing rough road', *Journal of Sound and Vibration*, Vol. 310, Nos. 1–2, pp.352–365.

Gupta, S., Ginoya, D., Shendge, P.D. et al. (2016) 'An inertial delay observer-based sliding mode control for active suspension systems', *Proceedings of the Institution of Mechanical Engineers, Part D: Journal of Automobile Engineering*, Vol. 230, pp.352–70.

Haddar, M., Chaari, R., Baslamisli, S.C. et al. (2021) 'Intelligent optimal controller design applied to quarter car model based on non-asymptotic observer for improved vehicle dynamics', *Proceedings of the Institution of Mechanical Engineers, Part I: Journal of Systems and Control Engineering*, Vol. 1, p.959651820958831.

Haemers, M., Derammelaere, S., Ionescu, C. et al. (2018) 'Proportional-integral state-feedback controller optimization for a full-car active suspension setup using a genetic algorithm', *IFAC-PapersOnLine*, Vol. 51, pp.1–6.

Hamada, Y. (2019) 'New LMI-based conditions for preview feedforward synthesis', *Control Engineering Practice*, Vol. 90, pp.19–26.

Jing, H., Wang, R., Li, C. et al. (2018) 'Robust finite-frequency H inf control of full-car active suspension', *Journal of Sound and Vibration*, Vol. 441, pp.221–239.

Kim, H.J., Seok Yang, H. and Park, Y.P. (2002) 'Improving the vehicle performance with active suspension using road-sensing algorithm', *Computers and Structures*, Vol. 80, Nos. 18–19, pp.1569–1577.

León-Vargas, F., Garelli, F. and Zapateiro, M. (2018) 'Limiting vertical acceleration for ride comfort in active suspension systems', *Proceedings of the Institution of Mechanical Engineers, Part I: Journal of Systems and Control Engineering*, Vol. 232, pp.223–232.

Nagarkar, M., Bhalerao, Y., Patil, G.V. and Patil, R.Z. (2018) 'Multi-objective optimization of nonlinear quarter car suspension system-PID and LQR control', *Procedia Manuf.*, Vol. 20, pp.420–427.

Paden, B., Cáp, M., Yong, S.Z., Yershov, D. and Frazzoli, E. (2016) 'A survey of motion planning and control techniques for self-driving urban vehicles', *IEEE Trans. Intell. Veh.*, Vol. 1, No. 1, pp.33–55.

Palli, S. and Koona, K. (2015) 'Analyses of dynamic response of a railway bogie', *Int. J. Vehicle Noise and Vibration*, Vol. 11, No. 2, pp.103–113.

Palli, S., Dontikurti, R., Sharma, R.C. and Sharma, N. (2021) 'Analysis of dynamic response of a railway locomotive using ANSYS', *Int. J. Vehicle Structures & Systems*, Vol. 13, No. 2, pp.250–255.

Pedro, J.O., Dangor, M., Dahunsi, O.A. et al. (2018) 'Dynamic neural network-based feedback linearization control of full-car suspensions using PSO', *Applied Soft Computing*, Vol. 70, pp.723–736.

Prabakar, R.S., Sujatha, C. and Narayanan, S. (2009) 'Optimal semi-active preview control response of a half car vehicle model with magnetorheological damper', *Journal of Sound and Vibration*, Vol. 326, Nos. 3–5, pp.400–420.

Qatu, M.S. (2012) 'Recent research on vehicle noise and vibration', *Int. J. Vehicle Noise and Vibration*, Vol. 8, No. 4, pp.289–301.

Qatu, M.S., Abdelhamid, M.K., Pang, J. and Sheng, G. (2009) 'Overview of automotive noise and vibration', *Int. J. Vehicle Noise and Vibration*, Vol. 5, Nos. 1/2, pp.1–35.

Sharma, R.C. (2017) 'Ride, eigenvalue and stability analysis of three-wheel vehicle using Lagrangian dynamics', *Int. J. Vehicle Noise and Vibration*, Vol. 13, No. 1, pp.13–25.

Sharma, R.C., Palli, S., Sharma, N. and Sharma, S.K. (2021a) 'Ride behaviour of a four-wheel vehicle using H infinity semi-active suspension control under deterministic and random inputs', *Int. J. Vehicle Structures & Systems*, Vol. 13, No. 2, pp.234–237.

Sharma, R.C., Sharma, S., Sharma, S.K., Sharma, N. and Singh, G. (2021b) 'Analysis of bio-dynamic model of seated human subject and optimization of the passenger ride comfort for three-wheel vehicle using random search technique', *Proc. Inst. Mech. Eng. Part K J. Multi-Body Dyn.*, Vol. 235, pp.106–121.

Sharma, S.K., Sharma, R.C. and Lee, J. (2021c) 'Effect of rail vehicle–track coupled dynamics on fatigue failure of coil spring in a suspension system', *Applied Sciences*, Vol. 11, No. 6, p.2650, Switzerland.

Sharma, R.C., Sharma, S.K., Sharma, N. and Sharma, S. (2020) 'Analysis of ride and stability of an ICF railway coach', *Int. J. Vehicle Noise and Vibration*, Vol. 16, Nos. 3/4, pp.127–144.

Sharma, S.K. and Sharma, R.C. (2019) 'Pothole detection and warning system for Indian roads', *Advances in Interdisciplinary Engineering, Proceedings of FLAME 2018*, pp.511–519.

Thompson, A.G. and Davis, B.R. (2003) 'RMS values of force, stroke and tyre deflection in a half-car model with preview controlled active suspension', *Vehicle System Dynamics*, Vol. 39, No. 3, pp.245–253.

Thompson, A.G. and Davis, B.R. (2005) 'Computation of the RMS state variables and control forces in a half-car model with preview active suspension using spectral decomposition methods', *Journal of Sound and Vibration*, Vol. 285, No. 3, pp.571–583.

Thompson, A.G. and Pearce, C.E.M. (2001) 'Performance index for a preview active suspension applied to a quarter-car model', *Vehicle System Dynamics*, Vol. 35, No. 1, pp.55–66.

Thompson, A.G. and Pearce, C.E.M. (2003) 'RMS values for force, stroke and deflection in a quarter-car model active suspension with preview', *Vehicle System Dynamics*, No. 1, pp.57–75.

Tseng, H.E. and Hrovat, D. (2015) 'State of the art survey: active and semi-active suspension control', *Vehicle System Dynamics*, Vol. 53, No. 7, pp.1034–1062.

Ulsoy, A.G., Peng, H. and Çakmakci, M. (2012) *Automotive Control Systems*, Cambridge University Press.

Wu, J., Liao, F. and Tomizuka, M. (2017) 'Optimal preview control for a linear continuous-time stochastic control system in finite-time horizon', *International Journal of Systems Science*, Vol. 48, pp.129–137.

Youn, I., Khan, M.A., Uddin, N. et al. (2017) 'Road disturbance estimation for the optimal preview control of an active suspension systems based on tracked vehicle model', *International Journal of Automotive Technology*, Vol. 18, pp.307–316.

Youn, I., Tchamna, R., Lee, S.H., Uddin, N., Lyu, S.K. and Tomizuka, M. (2014) 'Preview suspension control for a full tracked vehicle', *International Journal of Automotive Technology*, Vol. 15, No. 3, pp.399–410.